INTERNATIONAL JOURNAL OF EDUCATION AND INFORMATION TECHNOLOGIES
DOI: 10.46300/9109.2023.17.2 Volume 17, 2023

Modeling and Simulation of Faulty Induction Motor in DQ Reference Frame Using MATLAB/SIMULINK with MATLAB/GUIDE for Educational Purpose

Rohullah Rahmatullah[1,] Necibe Fusun Oyman Serteller [2,] Vedat Topuz [3]
[1,2] Marmara University, Faculty of Technology, Electrical and Electronics Engineering, Istanbul, Turkey
[3] Marmara University, Vocational School of Technical Sciences, Computer Technologies, Istanbul, Turkey

Received: June 26, 2022. Revised: January 13, 2023. Accepted: February 8, 2023. Published: March 13, 2023.

Abstract— Owing to their robust structure, induction motors are preferred to be used under difficult working conditions. Therefore, various faults may occur in the motor due to unexpected forces during the operations. Obtaining the data through experimental methods by physically creating faults in the induction motors, and analyzing their behavior is not efficient in terms of cost and time for educational purposes. Considering the above negative situation, in this paper, mathematical models have been developed in the dq0 stationary reference frame expressing three-phase stator windings short-circuit fault and broken rotor bar fault in induction motors. The proposed models are faster as compared to the other analytical models in terms of computation due to the rotor position independence of the inductance matrix. The faulty induction motor mathematical models have been implemented in the MATLAB/SIMULINK software environment with detailed explanations of each faulty model's subsystem. As a visual laboratory that can be used as an educational tool for the analysis of a three-phase faulty induction motor, a graphical user interface application has been developed in MATLAB/GUIDE, which allows users to simulate models from a single interface. As a case study, the behaviors of faulty induction motors in transient and steady states have been simulated in different severity scenarios of the faults. The park vector method has been used as a fault diagnosis approach to investigate fault types and the fault severity effects on the park vector pattern in each fault scenario. In addition, to observe the success of the developed Simulink toolboxes, they were used at Marmara University through courses in electrical machinery and evaluated by the graduated students at the end of the semester.

Keywords— Induction Motor, dq Reference Frame, Stator Fault, Rotor Fault, Park Vector, MATLAB/SIMULINK, MATLAB/GUIDE.

I. Introduction

Induction motors (IMs) have long been used in industrial applications where mechanical energy is required due to their robust structure and easy adaptability to various modes of operation in a dynamic state. Since IMs are mostly used in hard industrial environments, potential faults in the electrical or mechanical parts of the motor may occur because of exposure to unexpected forces during operation. In general, the stator and rotor structure of IM is designed to provide symmetrical characteristics, but faults that may occur for any reason break this symmetry. Asymmetries cause problems such as unbalanced air gap, voltages, and currents, increase in space and time harmonics, decrease in average torque, increase in pulses in the moment, increase in losses and decrease in efficiency, [1]. Faults in induction machines are commonly categorized as mechanical and electrical, of which electrical faults constitute 48% of the total faults. Frequently seen faults in induction machines used in industrial applications occur 38% in the stator and 10% in the rotor, [2]. There are many factors such as thermal, electrical, mechanical, and environmental stresses resulting in malfunctions in the stator and rotor. Generally, stator faults caused by insulation faults between two adjacent windings in the same phase are seen as stator windings short-circuit or open circuit, [3,4]. The thermal stress resulting in insulation degradation of windings is the main cause of stator winding faults, [5]. Other factors such as dielectric, corona, over currents and voltages, and transient voltages can also cause stator winding faults. Rotor faults are mainly caused by the cracking or breaking of rotor bars or end rings. The rotor faults are mainly developed from manufacturing defects, electromagnetic noises, centrifugal forces, oscillatory force, and aging of motor parts, [5,6].

To understand the behavior and performance of induction machines under different faults and develop reliable fault detection methods, accurate and simple models of faulty

induction machines are required. In literature, models for the simulation of induction machines with various faults are well investigated from simple T or π equivalent circuits to more complex ones such as Magnetic Equivalent Circuit (MEC), Finite-Element Method (FEM) and Multiple Coupled Circuit (MCC). The MEC model is based on the magnetic modeling of induction machines obtained by estimation of the network reluctances and permanence [7,8,9]. The FEM-based IM model is the most accurate model of IM by utilizing the magnetic and geometric characteristics of the machine to compute magnetic field distribution containing exact information on the stator, rotor, and mechanical part of the machine, [10,11].

The MCC models of induction machines with various faults are elaborated in [12,13], the model of the MCC-based faulty induction machine can be represented in three phases (abs) reference framework with the stator and rotor electrical equations and the mechanical equations of the machine. The main concept of the MCC model is based on the geometry and winding arrangement of the machines. In such models, machine inductances are evaluated using the winding function (WF). In, [14,15], harmonic effects for rotor slot design and a steady state modeling of stator faults are investigated with a generalized method of harmonic analysis. The transient model of induction machines for time-domain diagnosis of stator and rotor faults using the winding function approach is presented in, [16]. The same approach in [17], is used for frequency-domain diagnosis of poly-phase cage IM with inter-turn short-circuit in stator windings. The MCC-based model of IM with rotor faults is investigated in, [18,19], where the rotor cage is considered as a mesh by containing rotor and end ring loops.

The MCC-based model approach includes separate equations for each stator coil and rotor bar. It also encloses the mutual inductance terms being calculated in each numerical integration while solving model equations. Therefore, solving equations with simulation programs requires more time and memory capacity. To overcome this problem, more convenient and simpler models can be created in the dq0 reference frame system. dq0 reference frame theory is based on Clark and Park transformation where all variables of the machine from the neutral frame (three-phase system) are transformed into a two-phase system (dq0 system). Using the dq0 transformation, the number of equations is decreased, and all rotor position-dependent mutual inductances are made independent of the rotor position. Therefore, a simpler model of IM with stator and rotor faults can be obtained using the dq0 transformation theory. In, [20], stator windings short inter-turn fault modeling of IM in dq0 stationary reference frame is introduced and all parameters change due to fault are detailed. In, [21], a mathematical model was obtained in the dq0 reference frame for stator inter-turn short circuit fault in one phase, the developed model was simulated in MATLAB/SIMULINK environment for motors with different short-circuit percentages. In, [22,23], a dq0-based model approach in which the portion of short-circuit and the change of winding inductance in the stator is that to consider the leakage inductance to be proportional to square turns number was detailed just for short-circuit faults in one phase. A dq0 model of an induction machine with rotor faults was reported in, [24]. The modeling of healthy IM in the dq0 reference frame system and the latest information on modeling and evaluation of stator and rotor faults can be found in, [25,26].

This study focuses on developing models of IM that express stator short circuit faults in all three phases, in contrast to single-phase short-circuit faults in the stator windings, which are discussed extensively in the literature. The effects of broken rotor bars fault of IM have been modeled by unbalancing the rotor bar resistance. It is proposed to develop models of faulty IM that should be computationally faster than the MEC, FEM, MCC, and other analytical models in terms of simulating the behaviors of faulty IM. Therefore, to make the mathematical models of the faulty motor simple and independent of rotor position, all models have been built in the dq0 stationary reference frame system. In addition, to make the models usable for educational purposes, the derivation of all equations and implementation of the equations in the Simulink environment have been explained in detail. A MATLAB/GUIDE application has been developed to increase the usability of Simulink models developed for stator short-circuit fault and rotor broken bar fault of IM. Finally, the simulation result of the models under different severity levels of the faults has been displayed in the time domain.

II. STATOR AND ROTOR FAULT MODELS

Models to be developed for fault diagnosis and control of faulty IM must be of a form that will accurately reflect all behavior of the motor, but such a model will have an overly complex structure. Therefore, for simplicity, the following assumptions are considered:

- The stator windings are uniformly placed in the stator slots to create sinusoidal flux in the air gap.
- The magnetic circuit is linear, and saturation is neglected.
- Neglecting the effects of temperature and frequency changes on resistors and inductances.
- Permeability of the magnetic circuit is infinite.
- Neglecting hysteresis and eddy current losses.
- Neglecting tooth and slots effects.
- Neglecting current skin effect.

A. Modeling of stator short-circuit

The variation of the stator variables of IM directly depends on the winding number of phases a, b, and c. In general, the number of turns of the stator three phase-windings a, b, and c is designed structurally balanced and to be equal. However, a short circuit in the stator phase windings causes a decrease in the number of windings. Consequently, any short-circuit fault in stator windings results in a change for all the resistances and inductances of the stator windings. Therefore, a mathematical model is required which includes the variation of all stator phase resistance and inductance. If the percentage of short-circuit of phases a, b, and c are represented by K_{sa}^{*}, $K_{sb}{}^{*}$, and K_{sc}^{*}, respectively, the short-circuit coefficient for the

stator variable can be defined as below, [27].

$$\begin{aligned} K_{sa} &= 1 - K_{sa}^{*} \\ K_{sb} &= 1 - K_{sb}^{*} \\ K_{sc} &= 1 - K_{sc}^{*} \end{aligned} \quad (1)$$

Here, K_{sa}, K_{sb} and K_{sc} are the short-circuit coefficients for the stator variable in phases a, b, and c, respectively. $K_{sa}^{*} > 0$, $K_{sb}^{*} = 0$ and $K_{sc}^{*} = 0$ indicate that phase a is faulty and phases b and c are healthy. Therefore, if it is desired to examine a short-circuit fault in single phase a, the values of K_{sb}^{*} and K_{sc}^{*} are taken as zero. When there is a short-circuit in the stator phase windings, the diagonal matrix of the stator windings resistances $[R_s^{*}]$ can be defined using the short-circuit coefficients as the following equation:

$$\left[R_s^{*}\right] = \begin{bmatrix} R_s K_{sa} & 0 & 0 \\ 0 & R_s K_{sb} & 0 \\ 0 & 0 & R_s K_{sc} \end{bmatrix} \quad (2)$$

Similarly, the self-inductances $[L_S^{abs*}]$ of the stator phase windings can be arranged including the short-circuit effect as the following equation:

$$\left[L_s^{abc*}\right] = \begin{bmatrix} K_{sa}^2 (L_{1s} + L_{sm}) & K_{sa} K_{sb} L_{sm} & K_{sa} K_{sc} L_{sm} \\ K_{sa} K_{sb} L_{sm} & K_{sb}^2 (L_{1s} + L_{sm}) & K_{sb} K_{sc} L_{sm} \\ K_{sa} K_{sc} L_{sm} & K_{sc} K_{sb} L_{sm} & K_{sc}^2 (L_{1s} + L_{sm}) \end{bmatrix} \quad (3)$$

The mutual inductance matrices of stator-rotor and rotor-stator $[L_{sr}]$, $[L_{rs}]$ with the effect of short-circuit can be written in equation (4) and equation (5), respectively.

$$[L_{sr}^{abs*}] = L_{sr} \begin{bmatrix} K_{sa}cos(\theta_r) & K_{sa}cos(\theta_r + \frac{2\pi}{3}) & K_{sa}cos(\theta_r - \frac{2\pi}{3}) \\ K_{sb}cos(\theta_r - \frac{2\pi}{3}) & K_{sb}cos(\theta_r) & K_{sb}cos(\theta_r + \frac{2\pi}{3}) \\ K_{sc}cos(\theta_r + \frac{2\pi}{3}) & K_{sc}cos(\theta_r - \frac{2\pi}{3}) & K_{sc}cos(\theta_r) \end{bmatrix} \quad (4)$$

$$[L_{rs}^{abs*}] = L_{rs} \begin{bmatrix} K_{sa}cos(\theta_r) & K_{sb}cos(\theta_r - \frac{2\pi}{3}) & K_{sc}cos(\theta_r + \frac{2\pi}{3}) \\ K_{sa}cos(\theta_r + \frac{2\pi}{3}) & K_{sb}cos(\theta_r) & K_{sc}cos(\theta_r - \frac{2\pi}{3}) \\ K_{sa}cos(\theta_r - \frac{2\pi}{3}) & K_{sb}cos(\theta_r + \frac{2\pi}{3}) & K_{sc}cos(\theta_r) \end{bmatrix} \quad (5)$$

Since the mutual inductances between the stator and the rotor change according to the relative rotor position θ_r, it is more helpful to refer all the resistances and inductances matrices to the dq0 stationary reference frame system. The stator resistance matrix with short-circuit effect can be transferred to the dq0 stationary reference frame as in equation (6).

$$[R_s^{*qd0}] = \frac{2}{3} \begin{bmatrix} 1 & -\frac{1}{2} & -\frac{1}{2} \\ 0 & -\frac{\sqrt{3}}{2} & \frac{\sqrt{3}}{2} \\ \frac{1}{2} & \frac{1}{2} & \frac{1}{2} \end{bmatrix} \times \begin{bmatrix} K_{sa}R_s & 0 & 0 \\ 0 & K_{sb}R_s & 0 \\ 0 & 0 & K_{sc}R_s \end{bmatrix} \times \begin{bmatrix} 1 & 0 & 1 \\ -\frac{1}{2} & -\frac{\sqrt{3}}{2} & 1 \\ -\frac{1}{2} & \frac{\sqrt{3}}{2} & 1 \end{bmatrix} = \begin{bmatrix} R_{s11} & R_{s12} & R_{s13} \\ R_{s21} & R_{s22} & R_{s23} \\ R_{s31} & R_{s32} & R_{s33} \end{bmatrix} =$$

$$\begin{bmatrix} \frac{1}{6}R_s(4K_{sa} + K_{sb} + K_{sc}) & \frac{1}{2\sqrt{3}}R_s(K_{sb} - K_{sc}) & \frac{1}{3}R_s(2K_{sa} - K_{sb} - K_{sc}) \\ \frac{1}{2\sqrt{3}}R_s(K_{sb} - K_{sc}) & \frac{1}{2}R_s(K_{sb} + K_{sc}) & \frac{1}{\sqrt{3}}R_s(K_{sc} - K_{sb}) \\ \frac{1}{6}R_s(2K_{sa} - K_{sb} - K_{sc}) & \frac{1}{2\sqrt{3}}R_s(K_{sb} - K_{sc}) & \frac{1}{3}R_s(K_{sa} + K_{sb} + K_{sc}) \end{bmatrix} \quad (6)$$

Here, $[R_s^{*qd0}]$ is the matrix of stator resistances transferred to the dq0 stationary reference frame. Similarly, the stator inductances, stator-rotor inductances, and rotor-stator inductances are transferred to the dq0 stationary reference frame as the following expressions, respectively:

$$[L_s^{qd0*}] = [T(\theta = 0)][L_s^{abs*}][T(\theta = 0)]^{-1} = \begin{bmatrix} L_{s11} & L_{s12} & L_{s13} \\ L_{s21} & L_{s22} & L_{s23} \\ L_{s31} & L_{s32} & L_{s33} \end{bmatrix} \quad (7)$$

$$[L_{sr}^{qdo*}] = [T(\theta = 0)][L_{sr}^{abs*}][T(\beta)]^{-1} = \begin{bmatrix} L_{sr11} & L_{sr12} & L_{sr13} \\ L_{sr21} & L_{sr22} & L_{sr23} \\ L_{sr31} & L_{sr32} & L_{sr33} \end{bmatrix} \quad (8)$$

$$[L_{rs}^{qd0*}] = [T(\theta = 0)]^{-1}[T(\beta)][L_{rs}^{abs*}] = \begin{bmatrix} L_{rs11} & L_{rs12} & L_{rs13} \\ L_{rs21} & L_{rs22} & L_{rs23} \\ L_{rs31} & L_{rs32} & L_{rs33} \end{bmatrix} \quad (9)$$

Where $\left[L_s^{qd0*}\right]$, $\left[L_{sr}^{qd0*}\right]$ and $\left[L_{rs}^{qd0*}\right]$ are the inductance matrices of the stator, stator-rotor, and rotor-stator, respectively, transformed to dq0 reference frame, and their derivation is given in B-APPENDIX. Using all these new inductance matrices, the flux matrix $[\lambda]$ in the dq0 reference frame can be arranged as the following equation:

$$\begin{bmatrix} \lambda_s^q \\ \lambda_s^d \\ \lambda_s^0 \\ \lambda_r^q \\ \lambda_r^d \\ \lambda_r^0 \end{bmatrix} = \begin{bmatrix} L_{s11} & L_{s12} & L_{s13} & L_{sr11} & L_{sr12} & L_{sr13} \\ L_{s21} & L_{s22} & L_{s23} & L_{sr21} & L_{sr22} & L_{sr23} \\ L_{s31} & L_{s32} & L_{s33} & L_{sr31} & L_{sr32} & L_{sr33} \\ L_{rs11} & L_{rs12} & L_{rs13} & L_{1r} + L_m & 0 & 0 \\ L_{rs21} & L_{rs22} & L_{rs23} & 0 & L_{1r} + L_m & 0 \\ L_{rs31} & L_{rs32} & L_{rs33} & 0 & 0 & L_{1r} \end{bmatrix} \begin{bmatrix} i_s^q \\ i_s^d \\ i_s^0 \\ i_r^q \\ i_r^d \\ i_r^0 \end{bmatrix} \quad (10)$$

The stator and rotor voltage matrices (V_s, V_r) for the stator windings short-circuit fault in the stationary reference frame can be written as the following expressions, respectively:

$$\begin{bmatrix} v_s^q \\ v_s^d \\ v_s^0 \end{bmatrix} = \begin{bmatrix} R_{s11} & R_{s12} & R_{s13} \\ R_{s21} & R_{s22} & R_{s23} \\ R_{s31} & R_{s32} & R_{s33} \end{bmatrix} \begin{bmatrix} i_s^q \\ i_s^d \\ i_s^0 \end{bmatrix} + \frac{d}{dt} \begin{bmatrix} \lambda_s^q \\ \lambda_s^d \\ \lambda_s^0 \end{bmatrix} \quad (11)$$

$$\begin{bmatrix} v_r^q \\ v_r^d \\ v_r^0 \end{bmatrix} = \begin{bmatrix} R_r & 0 & 0 \\ 0 & R_r & 0 \\ 0 & 0 & R_r \end{bmatrix} \begin{bmatrix} i_r^q \\ i_r^d \\ i_r^0 \end{bmatrix} + \frac{d}{dt} \begin{bmatrix} \lambda_r^q \\ \lambda_r^d \\ \lambda_r^0 \end{bmatrix} + \begin{bmatrix} \lambda_r^q \\ \lambda_r^d \\ \lambda_r^0 \end{bmatrix} \begin{bmatrix} 0 & -\omega_r & 0 \\ \omega_r & 0 & 0 \\ 0 & 0 & 0 \end{bmatrix} \quad (12)$$

From the above equations, if the flux from equation (10) is placed in (11) and (12), in (13) the general voltage matrix system for stator windings short-circuit fault is obtained as the following formula:

$$\begin{bmatrix} v_s^q \\ v_s^d \\ v_s^0 \\ v_r^q \\ v_r^d \\ v_r^0 \end{bmatrix} = \begin{bmatrix} R_{11}+\frac{d}{dt}L_{s11} & R_{12}+\frac{d}{dt}L_{s12} & R_{13}+\frac{d}{dt}L_{s13} & \frac{d}{dt}L_{sr11} & \frac{d}{dt}L_{sr12} & \frac{d}{dt}L_{sr13} \\ R_{21}+\frac{dt}{d}L_{s21} & R_{22}+\frac{d}{dt}L_{s22} & R_{23}+\frac{d}{dt}L_{s23} & \frac{d}{dt}L_{sr21} & \frac{d}{dt}L_{sr22} & \frac{d}{dt}L_{sr23} \\ R_{31}+\frac{dt}{d}L_{s31} & R_{32}+\frac{d}{dt}L_{s32} & R_{33}+\frac{dt}{d}L_{s33} & \frac{d}{dt}L_{sr31} & \frac{d}{dt}L_{sr32} & \frac{d}{dt}L_{sr33} \\ \frac{d}{dt}L_{rs11}-\omega_r L_{rs21} & \frac{d}{dt}L_{rs12}-\omega_r L_{rs22} & \frac{d}{dt}L_{rs13}-\omega_r L_{rs23} & R_r+(L_{1r}+L_m) & -\omega_r(L_{1r}+L_m) & 0 \\ \frac{d}{dt}L_{rs21}+\omega_r L_{rs11} & \frac{d}{dt}L_{rs22}+\omega_r L_{rs12} & \frac{d}{dt}L_{rs23}+\omega_r L_{rs13} & \omega_r(L_{1r}+L_m) & R_r+(L_{1r}+L_m) & 0 \\ \frac{d}{dt}L_{rs31} & \frac{d}{dt}L_{rs32} & \frac{d}{dt}L_{rs33} & 0 & 0 & R_r+\frac{d}{dt}L_{1r} \end{bmatrix} \quad (13)$$

The symbol list and required derivations are given in APPENDIX A and B.

B. Modeling of induction motor with broken rotor bars

Broken rotor bars (BRBs) cause changes in rotor phase resistances and inductances. Thus, the current will decrease in phases with broken bars, and the current flowing from other healthy bars will increase, which will cause asymmetry of the current flowing through the rotor bars. The nonlinearity of the rotor current causes nonlinearity of the rotating magnetic field between the stator and the rotor, which causes frequency harmonics to be induced in the stator current, [23].

Rotor impedance inequality can be modeled by adding the impedance change ratio of the broken bars to the rotor phase resistances and inductances caused by the BRB. Since the change effect of rotor inductances is negligible beside the effect of rotor resistance. Therefore, it can be ignored and for a simpler mathematical model of the BRB fault, the assumptions that the rotor end ring contribution is neglected, and the stator phase inductances do not change can be used. The diagonal matrix of rotor resistance of a healthy and symmetrical IM in (abc) reference frame can be defined as follows:

$$R_r = \begin{bmatrix} R_{1r} & 0 & 0 \\ 0 & R_{1r} & 0 \\ 0 & 0 & R_{1r} \end{bmatrix} \quad (14)$$

The unbalanced rotor resistance $[R_r^*]$ effect can be included in the mathematical model of the motor by adding the change of resistance to the rotor phase resistance.

$$R_r* = \begin{bmatrix} R_{1r}+\Delta R_a & 0 & 0 \\ 0 & R_{1r}+\Delta R_b & 0 \\ 0 & 0 & R_{1r}+\Delta R_c \end{bmatrix} \quad (15)$$

Here ΔR_a, ΔR_b and ΔR_c represent the resistance change in phases a, b, and c as a result of the effect of broken bars, and can be evaluated as in equation (16), [28].

$$\Delta R_{abc} = R_r^* - R_r = \frac{3n_{bb}}{N_r - 3n_{bb}} R_r \quad (16)$$

where n_{bb} is the number of BRBs, N_r the total number of rotor bars, and R_r is the equivalent rotor resistance. Since we want to investigate the behavior of IM with BRBs in the stationary dq0 reference frame, we need to transform the rotor resistance matrix containing the broken bar portion to the dq0 reference frame. This transformation is obtained in equation (17) by multiplying the new rotor resistances matrix with the rotor dq0 transformation matrix.

$$[R_r^{qd0*}] = [T(\beta)][R_r^*][T(\beta)]^{-1} = \begin{bmatrix} R_{r11}+R_r & R_{r12} & R_{r13} \\ R_{r21} & R_{r22}+R_r & R_{23} \\ R_{r31} & R_{r32} & R_{r33}+R_r \end{bmatrix} \quad (17)$$

Here, $\left[R_r^{qd0*}\right]$ expresses the rotor resistance matrix of BRB faulty IM transformed to the dq0 reference frame, derived in APPENDIX-C. Using the $\left[R_r^{qd0*}\right]$ resistance matrix equation, the stator and rotor voltage matrices in the stationary reference frame with BRB fault can be defined by the following expressions:

$$\begin{bmatrix} v_s^q \\ v_s^d \\ v_s^0 \end{bmatrix} = \begin{bmatrix} R_s & 0 & 0 \\ 0 & R_s & 0 \\ 0 & 0 & R_s \end{bmatrix} \begin{bmatrix} I_s^q \\ I_s^d \\ I_s^0 \end{bmatrix} + \frac{d}{dt} \begin{bmatrix} \lambda_s^q \\ \lambda_s^d \\ \lambda_s^0 \end{bmatrix} \quad (18)$$

$$\begin{bmatrix} v_r^q \\ v_r^d \\ v_r^0 \end{bmatrix} = \begin{bmatrix} I_r^q \\ I_r^d \\ I_r^0 \end{bmatrix} \begin{bmatrix} R_{r11}+R_r & R_{r12} & R_{r13} \\ R_{r21} & R_{r22}+R_r & R_{23} \\ R_{r31} & R_{r32} & R_{r33}+R_r \end{bmatrix} + \frac{d}{dt} \begin{bmatrix} \lambda_r^q \\ \lambda_r^d \\ \lambda_r^0 \end{bmatrix} + \begin{bmatrix} \lambda_r^q \\ \lambda_r^d \\ \lambda_r^0 \end{bmatrix} \begin{bmatrix} 0 & -\omega & 0 \\ \omega & 0 & 0 \\ 0 & 0 & 0 \end{bmatrix} \quad (19)$$

If equations (18) and (19) are arranged in terms of currents, the general voltage matrix system for IM with BRB faults can be derived as the following formula:

$$\begin{bmatrix} v_s^q \\ v_s^d \\ v_s^0 \\ v_r^q \\ v_r^d \\ v_r^0 \end{bmatrix} = \begin{bmatrix} R_s + \frac{d}{dt}(L_{1s} + L_m) & 0 & 0 & \frac{d}{dt}L_m & 0 & 0 \\ 0 & R_s + \frac{d}{dt}(L_{1s} + L_m) & 0 & 0 & \frac{d}{dt}L_m & 0 \\ 0 & 0 & R_s + \frac{d}{dt}L_{1s} & 0 & 0 & 0 \\ \frac{d}{dt}L_m & -\omega_r L_m & 0 & R_r + R_{r11} + \frac{d}{dt}(L_{1r} + L_m) & R_{r12} - \omega_r(L_{1r} + L_m) & R_{r13} \\ \omega_r L_m & \frac{d}{dt}L_m & 0 & R_{r21} + \omega_r(L_{1r} + L_m) & R_r + R_{r22} + \frac{d}{dt}(L_{1r} + L_m) & R_{r23} \\ 0 & 0 & 0 & R_{r31} & R_{r32} & R_r + R_{r33} + \frac{d}{dt}L_{1r} \end{bmatrix} \begin{bmatrix} I_s^q \\ I_s^d \\ I_s^0 \\ I_r^q \\ I_r^d \\ I_r^0 \end{bmatrix} \quad (20)$$

III. MATLAB/SIMULINK IMPLEMENTATION

In this part of the study, the implementation of the obtained equations in MATLAB/SIMULINK environment is introduced, for this purpose, firstly it is necessary to rearrange the equations that have been obtained for stator short-circuit faulty and BRBs faulty IM to make them solvable with Matlab.

To develop the Simulink model for stator short circuit, the current equations from the voltage matrix system in equation (13) can be rearranged in terms of currents, and equations (21) to (26) which are applicable in the Simulink environment are obtained as following expressions:

$$\begin{aligned} i_s^q = \frac{1}{L_{s11}}\Big[\int \big[v_s^q - i_s^q R_{s11} - i_s^d R_{s12} - i_s^0 R_{s13}\big]\,dt \\ - \big(i_s^d L_{s12} + i_s^0 L_{s13} + i_r^q L_{sr11} \\ + i_r^d L_{sr12} + i_r^0 L_{sr13}\big)\Big] \end{aligned} \quad (21)$$

$$\begin{aligned} i_s^d = \frac{1}{L_{s22}}\Big[\int \big[v_s^d - i_s^q R_{s21} - i_s^d R_{22} - i_s^0 R_{s23}\big]\,dt \\ - (i_s^q L_{s21} + i_0^s L_{s23} + i_r^q L_{sr21} \\ + i_r^d L_{sr22} + i_r^0 L_{sr23})\Big] \end{aligned} \quad (22)$$

$$\begin{aligned} i_s^0 = \frac{1}{L_{s33}}\Big[\int \big[v_s^0 - i_s^q R_{s31} - i_s^d R_{s32} - i_s^0 R_{s33}\big]\,dt \\ - (i_s^q L_{s31} + i_s^d L_{s32} + i_r^q L_{sr31} \\ + i_r^d L_{sr32} + i_r^0 L_{sr33})\Big] \end{aligned} \quad (23)$$

$$\begin{aligned} i_r^q = \frac{1}{L_{1r} + L_m}\Big[\int \big[v_r^q - i_r^q R_r + \omega_r(i_s^q L_{rs21} + i_s^d L_{rs22} \\ + i_s^0 L_{rs23} + i_r^d(L_{1r} + L_m))\big]\,dt \\ - (i_s^q L_{rs11} + i_s^d L_{rs12} + i_0^s L_{rs13})\Big] \end{aligned} \quad (24)$$

$$\begin{aligned} i_r^d = \frac{1}{L_{1r} + L_m}\Big[\int \big[v_r^d - i_r^q R_r - \omega_r(i_s^q L_{rs11} + i_s^d L_{rs12} \\ + i_s^0 L_{rs13} + i_r^q(L_{1r} + L_m))\big]\,dt \\ - (i_s^q L_{rs21} + i_s^d L_{rs22} + i_0^s L_{rs23})\Big] \end{aligned} \quad (25)$$

$$\begin{aligned} i_r^0 = \frac{1}{L_{1r}}\Big[\int [v_r^0 - i_r^0 R_r]\,dt - (i_q^s L_{rs31} + i_s^d L_{rs32} \\ + i_s^0 L_{rs33})\Big] \end{aligned} \quad (26)$$

The implementation scheme of the mathematical model of the IM with a short-circuit fault in simulation programs is shown in Figure 1. Here, the inputs of the model are three-phase voltages, resistances, and inductances of the motor which are transferred to the dq0 reference frame.

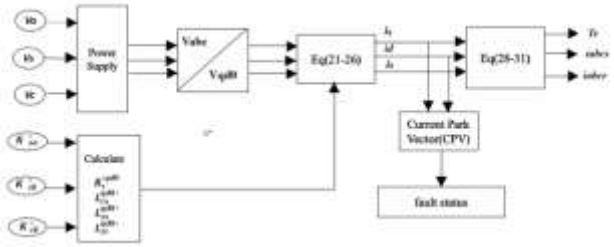

Fig. 1 Simulation flow chart of mathematical equations in d-q-0 reference frame for short-circuit IM

To build a general MATLAB/SIMULINK model for short-circuit faulty IM, all equations are implemented in the Simulink environment by constructing a subsystem of each equation. Firstly, the component of d-q-0-axis voltages is expressed as the following:

$$\begin{bmatrix} v_s^q \\ v_s^d \\ v_s^0 \end{bmatrix} = \frac{2}{3}\begin{bmatrix} cos(\theta) & cos\left(\theta - \frac{2\pi}{3}\right) & cos\left(\theta + \frac{2\pi}{3}\right) \\ sin(\theta) & sin\left(\theta - \frac{2\pi}{3}\right) & sin\left(\theta + \frac{2\pi}{3}\right) \\ \frac{1}{2} & \frac{1}{2} & \frac{1}{2} \end{bmatrix}\begin{bmatrix} v_{as} \\ v_{bs} \\ v_{cs} \end{bmatrix} \quad (27)$$

The subsystem Simulink model of equation (27) is represented in Figure 2, where the inputs of this block are the reference frame speed and three-phase voltage, and the outputs are dq-axis voltage components.

Fig. 2 Stator voltage conversion subsystem block

Figure 3 (a), (b), and (c) indicates the dq0 current subsystem blocks obtained by using equation (21) to equation (26), these blocks calculate d-q-0 current components.

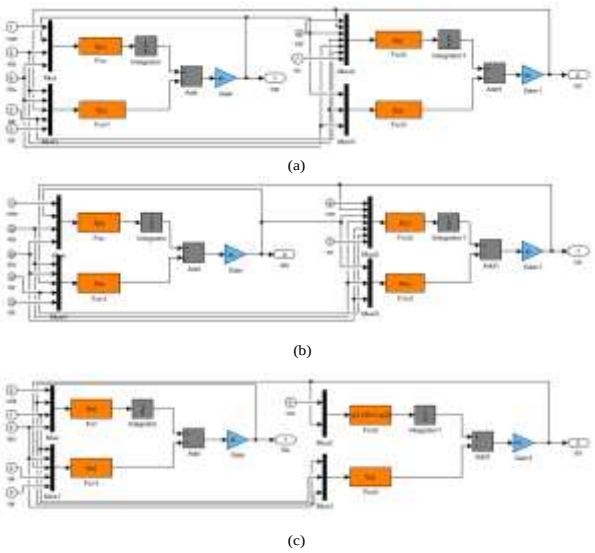

Fig. 3 (a) q-axis current subsystem block, (b) d-axis current subsystem block (c) zero current component subsystem block

In Figure 4, the Simulink block that calculates the torque and angular speed of the motor is obtained by using the torque equation (28) and the speed equation (29).

$$T_{EM} = \frac{3}{2}\frac{P}{2} L_m (i_r^d i_s^q - i_r^q i_s^d) \tag{28}$$

$$\omega_m = \frac{1}{J}\int (T_e - B\omega_m - T_L)\, dt \tag{29}$$

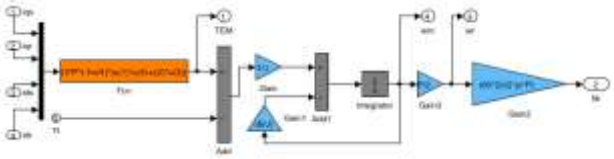

Fig. 4 Subsystem block calculating torque and rotor speed.

Finally, the stator and rotor current components of the dq-axis are transferred to the (abs) system by the following matrix equations, respectively:

$$\begin{bmatrix} v_{as} \\ v_{bs} \\ v_{cs} \end{bmatrix} = \begin{bmatrix} \cos(\theta) & \sin(\theta) & 1 \\ \cos\left(\theta - \frac{2\pi}{3}\right) & \sin\left(\theta - \frac{2\pi}{3}\right) & 1 \\ \cos\left(\theta + \frac{2\pi}{3}\right) & \sin\left(\theta + \frac{2\pi}{3}\right) & 1 \end{bmatrix} \begin{bmatrix} v_s^q \\ v_s^d \\ v_s^0 \end{bmatrix} \tag{30}$$

$$\begin{bmatrix} \mathrm{V_{ar}} \\ \mathrm{V_{br}} \\ \mathrm{V_{cr}} \end{bmatrix} = \begin{bmatrix} \cos(\beta) & \sin(\beta) & 1 \\ \cos\left(\beta - \frac{2\pi}{3}\right) & \sin\left(\beta - \frac{2\pi}{3}\right) & 1 \\ \cos\left(\beta + \frac{2\pi}{3}\right) & \sin\left(\beta + \frac{2\pi}{3}\right) & 1 \end{bmatrix} \begin{bmatrix} \mathrm{v_r^q} \\ \mathrm{v_r^d} \\ \mathrm{v_r^0} \end{bmatrix} \tag{31}$$

dq0-abc conversion blocks are shown in Figure 5, these blocks are developed using equations (30) and (31), which convert the dq0 stator and rotor current components to the (abs) system. The inputs of these blocks are dq0 stator and rotor currents and angular reference position, and their outputs are 3-phase stator and rotor currents.

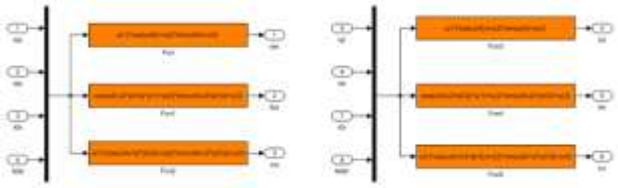

Fig. 5 dq0-abc conversion blocks

By masking the subsystem models, in Figure 6, a general MATLAB/SIMULINK model of IM with stator short-circuit is obtained. The inputs of the model are 3-phase voltages applied to the stator windings, the load torque, and the reference speed, while the outputs are three phase stator and rotor currents, rotor speed, and induced torque in the rotor.

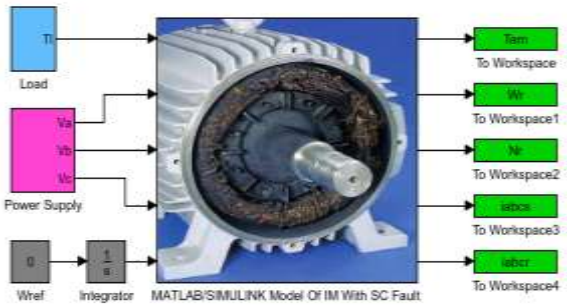

Fig. 6 A general MATLAB/SIMULINK model of stator short circuit IM

Likewise, to develop the Simulink model for BRBs fault, the current equations from the voltage matrix system in equation (20) can be rearranged and integration equations from equation (32) to (37) which can be implemented in the Simulink environment are obtained as following expressions:

$$\mathrm{i_s^q} = \frac{1}{\mathrm{L_{1s}} + \mathrm{L_m}} \left[\int \left(\mathrm{V_s^q} - \mathrm{i_s^q R_s} \right) dt - \mathrm{L_m i_r^q} \right] \tag{32}$$

$$\mathrm{i_s^d} = \frac{1}{\mathrm{L_{1s}} + \mathrm{L_m}} \left[\int (\mathrm{V_s^d} - \mathrm{i_s^d R_s}) \mathrm{dt} - \mathrm{L_m i_r^d} \right] \tag{33}$$

$$\mathrm{i_s^0} = \frac{1}{\mathrm{L_{1s}}} \int (\mathrm{V_s^0} - \mathrm{R_s i_s^0}) \mathrm{dt} \tag{34}$$

$$\mathrm{i_r^q} = \frac{1}{\mathrm{L_{1r}} + \mathrm{L_m}} \left[\int \left[\mathrm{V_r^q} - \mathrm{i_r^q (R_r + R_{11})} + \mathrm{i_r^d \omega_r (L_{1r} + L_m) - R_{21} i_r^d + \omega_r L_m i_s^d - i_r^0 R_{23}} \right] \mathrm{dt} - \mathrm{L_m i_s^q} \right] \tag{35}$$

$$\mathrm{i_r^d} = \frac{1}{\mathrm{L_{1r}} + \mathrm{L_m}} \left[\int \left[(\mathrm{V_r^d} - \mathrm{i_r^d (R_r + R_{22})} - \mathrm{i_r^q \omega_r (L_{1r} + L_m) - R_{21} i_r^q - \omega_r L_m i_r^d - i_r^0 R_{23}} \right] \mathrm{dt} - \mathrm{L_m i_s^d} \right] \tag{36}$$

$$\mathrm{i_r^0} = \frac{1}{\mathrm{L_{1r}}} \int [\, \mathrm{V_r^0} - (\mathrm{R_r + R_{33}}) \mathrm{i_r^0} - \mathrm{i_r^q R_{31}} - \mathrm{i_r^d R_{23}}] \mathrm{dt} \tag{37}$$

The implementation scheme to build the Simulink model of IM with BRBs fault is detailed in Figure 7. As a flowchart, firstly rotor resistances are transferred to the dq0 reference plane by using equation (17) and 3-phase voltage is transferred to the dq0 reference frame with the help of equation (27).

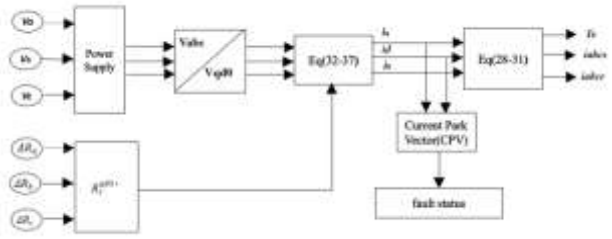

Fig. 7 Simulation flowchart for broken rotor bars faulty IM

The implementation of equations (32) to (37), which calculate the dq0 current components of the stator and rotor are carried out by constructing subsystem blocks respectively in Figure 8(a), (b), and(c).

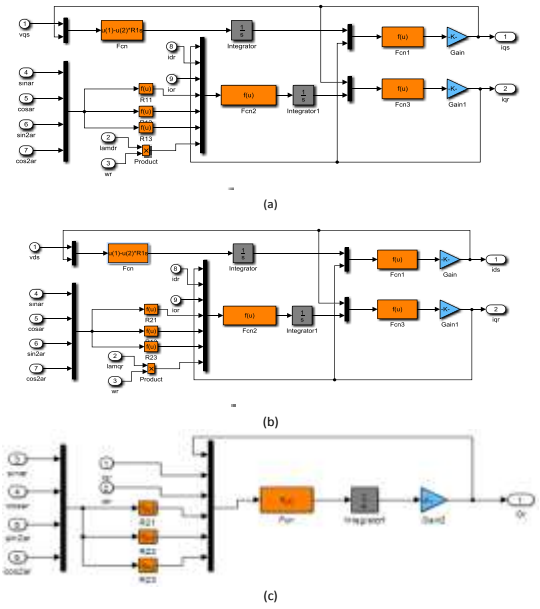

Fig. 8 (a) q-axis currents subsystem block, (b) d-axis currents subsystem block (c) zero current component subsystem block

IV. MATLAB/GUIDE IMPLEMENTATION

To make the developed Simulink models more usable for educational purposes, a Graphical User Interface Development Environment (GUIDE) of Matlab software shown in figure 9 has been developed. This MATLAB/GUIDE application makes it easy for the user to simulate models created for faulty IM on the same platform. The mentioned GUI application consists of 'Healthy IM', `IM with unbalanced stator', and 'IM Broken Rotor Bar' interfaces.

Figure 9 presents the 'IM healthy' state consisting of the 'parameters panel', 'power supply panel', and 'load panel'. By using the 'IM healthy' interface, motor parameters, power supply, and load data can be defined to both stator short-circuit faulty and BRBs faulty IM Simulink models. The 'Healthy IM' interface allows the user to easily simulate machines of different power. Users have access to change the applied voltage, motor load and motor parameters, and investigate the change effects of load and motor parameters on the motor torque and speed behaviors. The user also can observe the d and q current and voltage components variation of the motor in the stationary, rotor, and synchronous reference frame system.

Fig. 9 'Healthy IM' main interface.

Figure 10 shows the IM unbalanced stator state, by using this state the behaviors of IM with stator unbalanced voltages, voltage phase angles or stator short-circuit fault can be examined separately in one phase or all three phases. Here the simulation results of the faulty model can be visually investigated in the time domain or can be presented in the current park vector pattern.

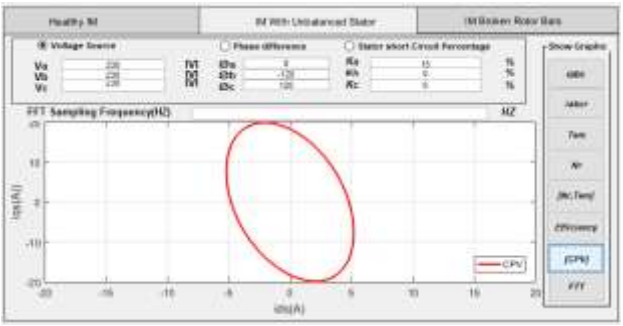

Fig. 10 Main interface for IM with Unbalanced Stator

Figure 11 demonstrates the 'IM broken rotor bar' interface page developed for the Simulink model of IM with BRB fault. By using this interface, the behavior of IM with a different number of BRBs can be simulated in the time domain or the effect of BRBs can be investigated in the current park vector pattern.

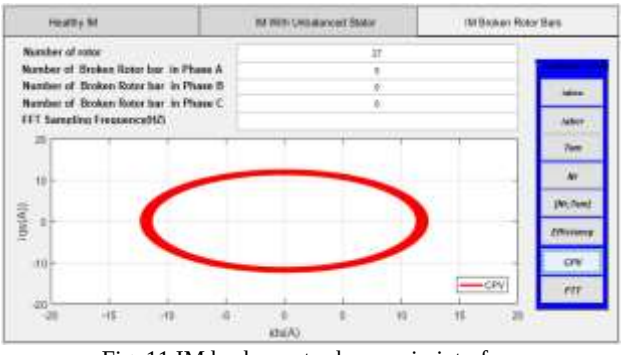

Fig. 11 IM broken rotor bars main interface

The simulation process of developed Simulink models with MATLAB/GUIDE is represented in Figure 12, here firstly the motor parameter, load, and three-phase voltage data are defined from the main page to the Simulink models, then the fault data of stator short-circuit, or broken rotor can be introduced to related Simulink model. Finally, the simulation results can be visualized by clicking on buttons taking part in the 'show graphic' panel.

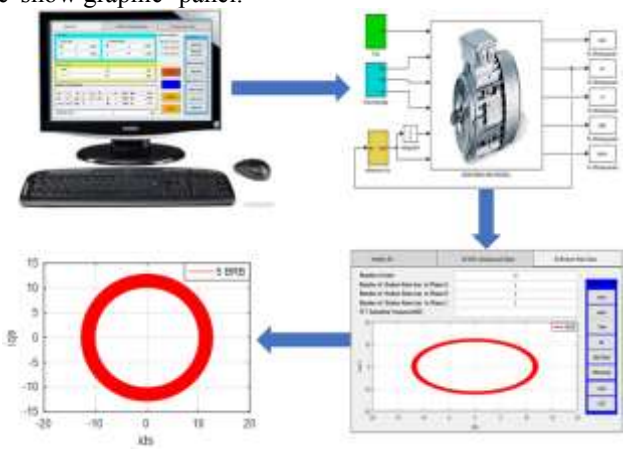

Fig. 12 MATLAB/GUIDE workflow

V. Simulation Results and Students Feedback

This section of the study represents the simulation results of developed Simulink models of faulty IM under different severity of the faults both in the time domain and in the park vector pattern. Then the students' comments and evaluations about the work have been explained. Firstly, Simulation results for the motor parameters, given in D-APPENDIX are carried out by using the Simulink model developed for the motor with the stator windings short-circuit. In Figure 13, the simulation output of stator phase currents in case of a 3% short-circuit fault in phase a is shown, and it is seen that the current in the faulty phase has been raised.

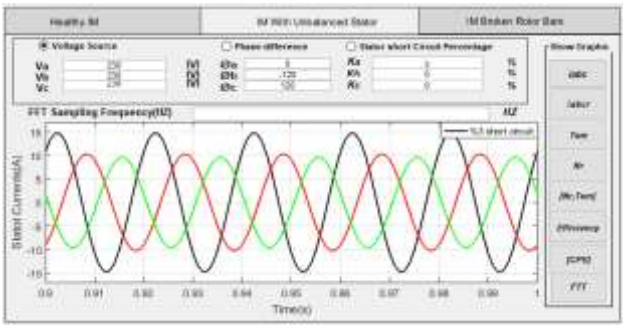

Fig. 13 Simulation output of stator phase currents for 3% short-circuit fault in phase a.

Figure 14 (a), (b), (c), and (d) demonstrate the variation of stator currents, torque, speed, and speed-torque behavior under healthy, 5%, 10%, and 15 % short-circuit faults in phase a, respectively. Due to the unbalanced current in the stator phases, the formation of the unbalanced field occurs, which forces the motor to rotate in positive and negative directions. Thus, it is observed that oscillations occur in the speed and torque waves, and the amplitudes of the oscillations increase with the increase of the fault.

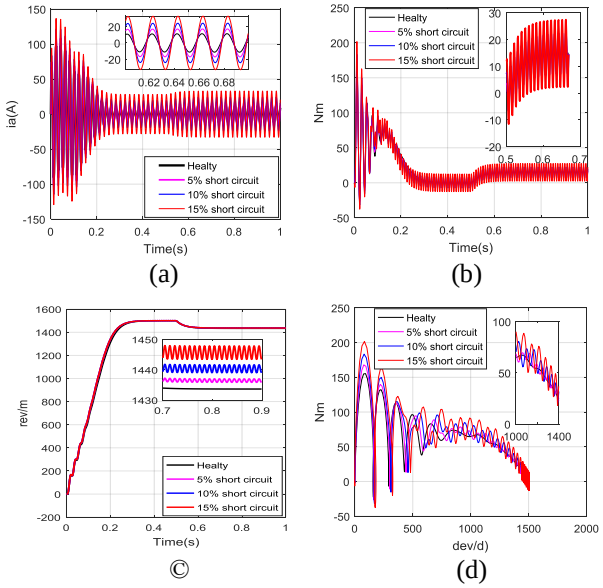

Fig.14 Simulation output of healthy,5 %, 10% and 15% short-circuit faults in phase a, under full load after 0.5s, (a) phase currents, (b) torque, (c) speed, (d) speed torque

Figure 15 (a) indicates the current park vector patterns drawn separately for healthy, 10% short-circuit fault in phase a, 10% short-circuit fault in phase b, and 10% short-circuit fault in phase c. In healthy conditions, the current park vector pattern is circular, in faulty conditions elliptical distortion occurs in the shape of the pattern, and the current park pattern takes place at different angles with the y-axis for faults individual in phases a, b, and c. Figure 15 (b) shows the current park vector pattern obtained for healthy, 5 %, 10%, and 15% short-circuit faults in the stator phase a. A rising in fault causes an increase in the major radius of the ellipse and a decrease in the minor radius. In healthy conditions, the radius of the circle is 11 units and fixed to the coordinate center. In case of 5 %, 10%, and 15% short-circuit fault in the stator phase a, the respective length of the major axis of the elliptical current park vector pattern becomes 13-unit,16 units and 19 units, and in all fault cases in phase a, the pattern is located at the angle of 50° with the y-axis.

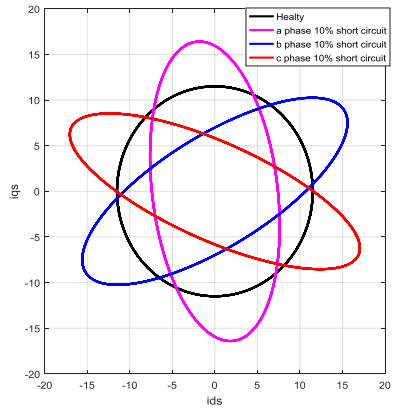

(a)

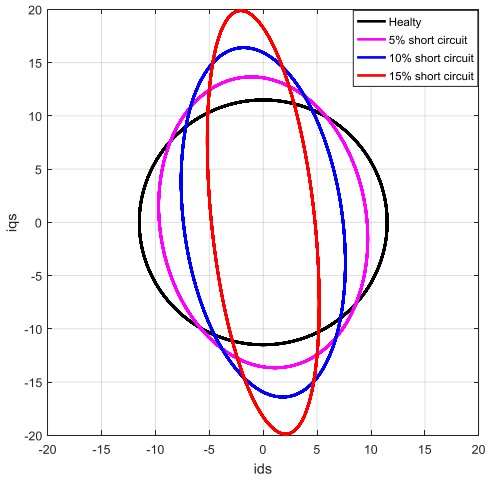

(b)

Fig. 15 Current Park vector patterns:(a) Healthy, %10 stator short circuit in phases a, b, and c, (b) phase a healthy, %5, %10, %15 short-circuit fault.

To examine the behavior of BRB faulty IM, the motor parameters given in D-APPENDIX have been tested on the Simulink model developed for BRB faulty condition. Simulation results are obtained for the presence of 1BRB, 3BRB, and 5 BRB faults. If the rotor bar is broken in the motor, there is no symmetry in the magnetic field between the stator and the rotor. Since no current flows on the broken rotor bars, deterioration occurs in the stator and rotor currents. Figure 16 demonstrates the variation of the stator phase current in healthy, 1BRB, 3BRB, and 5BRB fault conditions. It is seen that there is a deterioration in the form of the current signal due to the fault and increases with the fault rising.

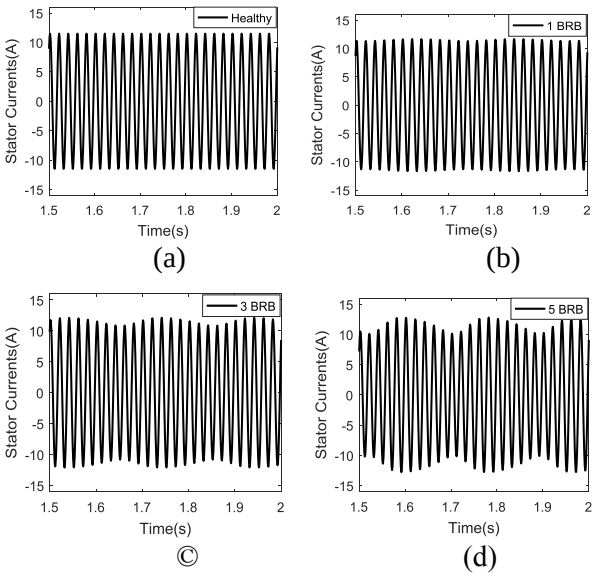

(a) (b) © (d)

Fig. 16 Simulation output for the stator phase a current in case of healthy 1BRB, 3BRBand 5BRB.

Figure 17 indicates the transient and steady-state behavior of IM under full load after 0.5s in the case of healthy, 1BRB, 3BRB and 5BRB faults. Contrary to the healthy state, fluctuations occur in the torque and speed signals both in the transient and steady-state region, and fluctuation increases with rising the number of BRBs. However, it has been observed that the average speed values decreased with the increasing number of BRBs.

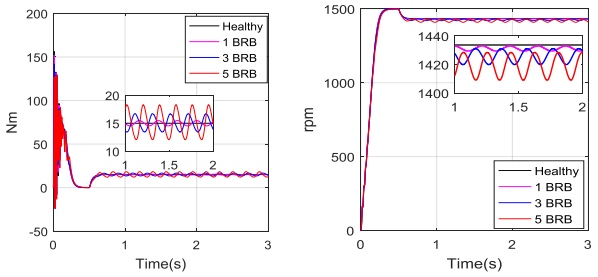

(a) (b)

Fig. 17 Simulation output for the stator phase a current in case of healthy, 1 BRB, 3 BRB and 5 BRB, (a) torque, (b) speed

Figure 18 indicates the current park vector modules obtained by using the steady state values of i_s^q and i_s^d current components in case of healthy, 1BRB, 3BRB, and 5BRB faults. The resulting current park vector module for healthy IM is a complete circle. The current park vector modules obtained in the case of 1BRB, 3BRB, and 5BRB are in the form of a ring and it is seen that the thickness of the ring increases with the severity of the fault.

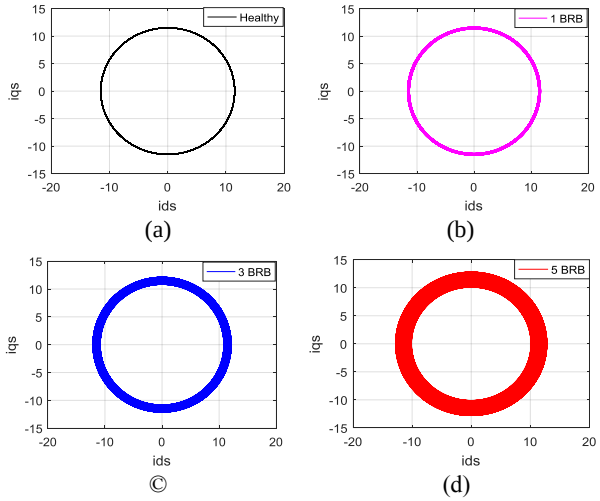

(a) (b) © (d)

Fig .18 Current Park vector Patterns in case of (a) healthy, (b) 1BRB, (c) 3BRB, (d) 5BRB

VI. Educational Issues and Assessment Results

The study of faulty IM based on MATLAB/Simulink software has been successfully used in several courses. In Marmara University at the graduate level, the developed Simulink models were used in the courses Design of Electric Machines and Transient States in Electrical Machines given in the semesters 2019-2020 and 2020-2021 covering a total 31 of students.

The basic concept of the dq0 reference frame systems, three-phase to two-phase conversion, and stationary and synchronous reference frames have been detailed with

necessary explanations throughout the course. After learning the dq0 transformation (Clark Transformation), it was applied to a three-phase healthy IM mathematical model and transformed to the qd0 arbitrary reference frame. The mathematical model of the IM motor in qd0 arbitrary reference frame was implemented in the Simulink environment and the d and q voltage and current components were simulated in stationary reference, rotor reference, and synchronous reference frame systems by changing the arbitrary reference speed equal to stationary(zero) speed, rotor speed and synchronous speed, respectively. The transient and steady-state behaviors of motors under the different load conditions in a healthy state were examined during the healthy motor modeling subject. The study related to healthy IM can be found in, [25].

After reinforcing the mathematical modeling of the healthy IM and its behaviors, the stator and rotor faulty IMs were modeled in the dq0 stationary reference frame and implemented in the Simulink environment. The stator and rotor faulty models were tested by students during the lesson. The effects of each fault and the severity of each fault on the stator current, speed, and torque were observed in the time domain. In addition, the data from the simulation results in the case of each fault was recorded and for each fault scenario, the park vector pattern was analyzed.

At the end of the semesters, the dq frame and faulty IM modeling by using Simulink and simulation with MATLAB/GUIDE were assessed by MSc students in two different semester course materials under five categories called A, B, C, D, and E. In A category, the students were asked to score the simplicity of modeling of a faulty IM in the dq0 reference frame system,89.5% of students evaluated as positive, and 10.5% gave negative scores due to not considering some parameters such as skin effects or saturation problems in mathematical models. In the B category, students were asked to score the implementation of the mathematical models under the MATLAB/SIMULINK environment, 96% of them found it practical while 4% of them thought that the models are complex to be used for education purposes. In the C category, they were asked to assess the simulation result viewability using the MATLAB/GUIDE application developed for Simulink models,94.5% of their feedback was positive and 5.5% of them recommended adding more options to the mentioned GUI application. In the D category, the students were requested to evaluate the dynamic behaviors of faulty IM in the time domain under different fault severity scenarios, 70% of the participants gave positive scores and the rest of them thought that it is difficult to distinguish faults from each other in the time domain. In the E category, the students participated in the evaluation of fault analysis by using the current park vector method. Approximately %98.5 of the students were of the same opinion that the current park vector is the optimal method that can reflect the fault type and fault severity in a more distinguishable manner.

The assessment results are summarized in Table 1 and the average of all observations through the two-semester courses is represented in figure 19. According to the results of the evaluation of the students, models of the faulty models in the dq0 reference frame attract attention in electrical machinery lessons due to advantages such as reduction of mathematical equations, independence of inductance expressions from rotor position, simplicity of models, easy design in Simulink environment and less simulation time. The main disadvantage of the faulty IM models in the dq0 reference frame, pointed out by the students, is that the models obtained for the motor do not include some parameters effects such as current skin effect, hysteresis and Foucault's losses, temperature and frequency effects, and magnetic circuit effects. In general, from the student evaluations on the faulty IM dq0 models, we can conclude that the model can be used for modeling faulty IM, ignoring some parameters that do not affect the motor behaviors much under normal operating conditions. However, if one works on an IM design, the effects of the parameters should be included in the mathematical models according to the importance of the study.

TABLE 1 Summary of Assessed Data over two semesters.

Assessed Data		**Group.1**	**Group.2**
Semester		2019 Fall	2020 Fall
Number of students		15	16
Category	**Score**	Out of 100	Out of 100
A	Simplicity of modeling of a faulty induction motor in dq reference frame system	89	90
B	Implementation of the mathematical models in MATLAB/SIMULINK environment	95	97
C	Simulation viewability using MATLAB/GUIDE application	98	91
D	Behavior of faulty induction motor in time domain under different fault severity scenario	67	73
E	Fault analysis by using current park vector method	98	99
Total Score		89.4	90

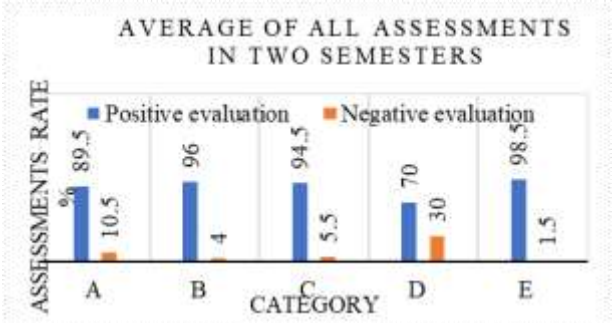

Fig. 19 Average of all assessments in two semesters

During the course face to face, the questionnaire has been realized to measure the effectiveness of using MATLAB/GUIDE simulation actively in electric machine theory courses. The master science students in Marmara University, Electric-Electronic Engineering department have participated in this study. They remarked that the learning of mathematical models and fault analysis of IM with the visual expressions using the MATLAB/SIMULINK environment as a software laboratory with its features in the electric machine course reinforced their understanding of theoretical knowledge and increased their interest in the subject matter. As for the validity of the models, the simulation results obtained from the developed models were found close to the experimental results, so the course teacher and the students suggested that the models can be used as the stator short circuit faults and rotor faults data generator. The faulty models can be simulated for any desired simulation time and any specified fault severity, and the data of the motor torque or stator currents can be recorded for the use of developing classic fault diagnosis methods or artificial intelligence-based methods for fault control and diagnosis. Moreover, the models created under the Simulink software environment can be used by students as a virtual laboratory during the lesson to understand the behaviors of IM during healthy and faulty conditions.

VII. CONCLUSION

Developing an accurate faulty IM model that accurately represents the dynamic behavior of the faults and hence developing an appropriate fault detection and control method is important for both education and practical applications. However, a comprehensive and complex model is required to accurately represent the fault behavior, which will have limitations in both model building and simulation time. In this study, a dq-based approach is used for obtaining more simplified models expressing stator three-phase short-circuit fault and BRB fault compared to previous studies focusing only on single-phase faults. To use the models for educational purposes the derivation and arrangement of all equations and their implementation in the Simulink environment have been clearly explained. To increase the usability of faulty IM Simulink models developed for educational purposes, a MATLAB GUI application has been designed that can provide access to all models and display simulation outputs from a single interface. By using the proposed GUI, the user can simulate motors of different power with different loads under the condition of healthy, stator short circuit fault and BRB fault. The scenarios created in the Simulink software environment are arranged in a way that allows students to use and develop them in a virtual laboratory in lessons so that they can understand the behaviors of IM in healthy and faulty situations in detail. The developed models of faulty IM and the educational tools are suitable for higher education students engaged in IM faults analysis and simulation.

As a result of the validation of the models to test the healthy and faulty IM Park Vector pattern, the models were simulated under healthy and faulty conditions and the recorded data of q and d current components was used for investigating the effects of each fault and its severity on the park vector pattern. The park vector module obtained for the healthy motor was observed in the shape of a circle. In the case of a short-circuit fault in each of the three phases individually, the park vector patterns have been seen in the same elliptical shape but located at different angles to the y-axis. It has been observed that a short-circuit fault rising in single phase results in an increase in the major axis of the ellipse and a decrease in the minor axis. In the case of the BRB fault, the current park vector pattern has been observed in the shape of a ring, and it was noticed that the thickness of the ring increased with the increase in the BRB number.

APPENDIX

A-APPENDIX: Symbols

T_L	Load moment (Nm)
T_e	Induced moment (Nm)
L_{1s} , L_{1r}	Rotor and stator leakage inductances(H)
L_m	Magnetization inductance((H)
f_s	Source frequency(f)
i_s^q , i_s^d , i_s^0	Stator current components(A) in the qd0 reference frame
i_r^q , i_r^d , i_r^0	Rotor current components(A) in the qd0 system
λ_s^q , λ_s^d , λ_s^0	Stator flux connections (Wb) in the qd0 system
λ_r^q , λ_r^d , λ_r^0	Rotor flux connections (Wb) in the qd0 system
v_s^q , v_s^d , v_s^0	Stator voltage components(V in the qd0 system
v_r^q , v_r^d , v_r^0	Rotor voltage components(V) in the qd0 system

B -APPENDIX:

L_s^{qd0*}, L_{rs}^{qd0*} and L_{sr}^{qdo*} derivation.

$$L_s^{qd0*} = [T(\theta=0)]\left[L_s^{abs*}\right][T(\theta=0)]^{-1}$$

This equation can be written in the stationary reference plane as below.

$$\frac{2}{3}\begin{bmatrix} 1 & -\frac{1}{2} & -\frac{1}{2} \\ 1 & -\frac{\sqrt{3}}{2} & \frac{\sqrt{3}}{2} \\ \frac{1}{2} & \frac{1}{2} & \frac{1}{2} \end{bmatrix} \times \begin{bmatrix} K_a{}^2(L_{1s}+L_m) & K_aK_{sb}L_m & K_{sa}K_{sc}L_m \\ K_aK_{sb}L_m & K_b{}^2(L_{1s}+L_m) & K_{sb}K_{sc}L_m \\ K_aK_{sc}L_m & K_{sc}K_{sb}L_m & K_{sc}{}^2(L_{1s}+L_m) \end{bmatrix} \times \begin{bmatrix} 1 & 0 & 1 \\ -\frac{1}{2} & -\frac{\sqrt{3}}{2} & 1 \\ -\frac{1}{2} & \frac{\sqrt{3}}{2} & 1 \end{bmatrix} = \begin{bmatrix} L_{s11} & L_{s12} & L_{s13} \\ L_{s21} & L_{s22} & L_{s23} \\ L_{s31} & L_{s32} & L_{s33} \end{bmatrix}$$ when simplified.

$$L_{s11=}\frac{1}{6}l_{1s}(4K_a^2+K_b^2+K_c^2)+\frac{1}{9}l_m(4K_a^2+K_b^2+K_c^2+2K_aK_b+2K_aK_{cc}-K_bK_c)$$

$$L_{s12=}\frac{\sqrt{3}}{6}l_{1s}(K_b^2-K_c^2)+\frac{\sqrt{3}}{9}l_m(K_b^2-K_c^2)$$

$$L_{s13} = \frac{1}{3} l_{1s}(4K_a^2 - K_b^2 - K_c^2) + \frac{1}{9} l_{ms}(4K_a^2 - 2K_b^2 - 2K_c^2 - 2K_aK_b - K_aK_{cc} + 2K_bK_c)$$

$$L_{s21=} \frac{\sqrt{3}}{6} l_{1s}(K_b^2 - K_c^2) + \frac{\sqrt{3}}{9} l_m K_b^2 - K_c^2)$$

$$L_{s22=} \frac{1}{2} l_{1s}(K_a^2 + K_b^2) + \frac{1}{3} l_m(K_a^2 + K_b^2 + K_c^2 + K_bK_c)$$

$$L_{s32=} \frac{\sqrt{3}}{6} l_{1s}(K_c^2 - K_b^2) + \frac{\sqrt{3}}{6} l_m(2K_c^2 - 2K_c^2 + K_aK_b - 2K_aK_c)$$

$$L_{s31} = \frac{1}{6} l_{1s}(2K_a^2 - K_b^2 - K_c^2) + \frac{1}{18} l_m(4K_a^2 - 2K_b^2 - 2K_c^2 - 2K_aK_b - K_aK_{cc} + 2K_bK_c)$$

$$L_{s32=} \frac{\sqrt{3}}{6} l_{1s}(K_b^2 - K_c^2) + \frac{\sqrt{3}}{18} l_m(2K_c^2 - 2K_b^2 + K_aK_b - K_aK_c)$$

$L_{s33=} \frac{1}{3} l_{1s}(K_a^2 + K_b^2 + K_c^2) + \frac{2}{9} l_m(K_a^2 + K_b^2 + K_c^2 - 2K_aK_b - 2K_aK_{cc} - K_bK_c)$ are obtained.

$L_{sr}^{qdo*} = [T(\theta = 0)][L_{sr}^{abs*}][T(-\theta_r)]^{-1}$ This equation can be written in the stationary reference plane as below.

$$\frac{2}{3}\begin{bmatrix} 1 & -\frac{1}{2} & -\frac{1}{2} \\ 1 & -\frac{\sqrt{3}}{2} & \frac{\sqrt{3}}{2} \\ \frac{1}{2} & \frac{1}{2} & \frac{1}{2} \end{bmatrix} L_{sr} \begin{bmatrix} K_a cos(\theta_r) & K_a cos\left(\theta_r + \frac{2\pi}{3}\right) & K_a cos\left(\theta_r - \frac{2\pi}{3}\right) \\ K_b cos\left(\theta_r - \frac{2\pi}{3}\right) & K_b cos(\theta_r) & K_b cos\left(\theta_r + \frac{2\pi}{3}\right) \\ K_c cos\left(\theta_r + \frac{2\pi}{3}\right) & K_c cos\left(\theta_r - \frac{2\pi}{3}\right) & K_c cos(\theta_r) \end{bmatrix} \times \begin{bmatrix} cos(-\theta_r) & sin(-\theta_r) & 1 \\ cos(-\theta_r - \frac{2\pi}{3}) & sin(-\theta_r - \frac{2\pi}{3}) & 1 \\ cos(-\theta_r + \frac{2\pi}{3}) & sin(-\theta_r + \frac{2\pi}{3}) & 1 \end{bmatrix} = \begin{bmatrix} L_{sr11} & L_{sr12} & L_{sr13} \\ L_{sr21} & L_{sr22} & L_{sr23} \\ L_{sr31} & L_{sr32} & L_{sr33} \end{bmatrix}$$

When this matrix equation is simplified

$$L_{sr11} = \frac{1}{6} l_m(4K_a + K_b + K_c)$$

$$L_{sr12} = \frac{\sqrt{3}}{6} l_m(K_b - K_c)$$

$$L_{sr13} = 0$$

$$L_{sr21} = \frac{\sqrt{3}}{6} l_m(K_b - K_c)$$

$$L_{sr22} = \frac{1}{2} l_m(K_b + K_c)$$

$$L_{sr23} = 0$$

$$L_{sr31} = \frac{1}{6} l_m(2K_a - K_b - K_c)$$

$$L_{sr32} = \frac{\sqrt{3}}{6} l_m(K_{cc} - K_b)$$

$L_{sr33} = 0$. are obtained.

$L_{rs}^{qd0*} = [T(\beta)][L_{sr}^{abs}][T(\beta)]^{-1}$ This equation can be written in the stationary reference plane as below.

$$\begin{bmatrix} \cos(\theta) & \cos\left(-\theta_r - \frac{2\pi}{3}\right) & \cos\left(-\theta_r + \frac{2\pi}{3}\right) \\ \sin(-\theta_r) & \sin\left(-\theta_r - \frac{2\pi}{3}\right) & \sin\left(-\theta_r + \frac{2\pi}{3}\right) \\ \frac{1}{2} & \frac{1}{2} & \frac{1}{2} \end{bmatrix} L_{rs} \times \begin{bmatrix} K_a \cos(\theta_r) & K_b \cos\left(\theta_r - \frac{2\pi}{3}\right) & K_c \cos\left(\theta_r + \frac{2\pi}{3}\right) \\ K_a \cos\left(\theta_r + \frac{2\pi}{3}\right) & K_b \cos(\theta_r) & K_c \cos\left(\theta_r - \frac{2\pi}{3}\right) \\ K_a \cos\left(\theta_r - \frac{2\pi}{3}\right) & K_b \cos\left(\theta_r + \frac{2\pi}{3}\right) & K_c \cos(\theta_r) \end{bmatrix} L_{rs} \times \begin{bmatrix} cos(-\theta_r) & sin(-\theta_r) & 1 \\ cos(-\theta_r - \frac{2\pi}{3}) & sin(-\theta_r - \frac{2\pi}{3}) & 1 \\ cos(-\theta_r + \frac{2\pi}{3}) & sin(-\theta_r + \frac{2\pi}{3}) & 1 \end{bmatrix} = \begin{bmatrix} L_{rs11} & L_{rs12} & L_{rs13} \\ L_{rs21} & L_{rs22} & L_{rs23} \\ L_{rs31} & L_{rs32} & L_{rs33} \end{bmatrix}$$

When this equation is simplified

$$L_{rs11} = \frac{1}{6} l_m(4K_a + K_b + K_c)$$

$$L_{rs12} = \frac{\sqrt{3}}{6} l_m(K_b - K_c)$$

$$L_{rs13} = \frac{1}{6} l_m(2K_a - K_b - K_c)$$

$$L_{rs21} = \frac{\sqrt{3}}{6} l_m(K_b - K_c)$$

$$L_{rs22} = \frac{1}{2} l_m(K_b + K_c)$$

$$L_{rs23} = \frac{\sqrt{3}}{6} l_m(K_{cc} - K_b)$$

$L_{rs13} = L_{rs33} = L_{rs33} = 0$ are obtained.

C-APPENDIX:

$$R_{r11} = \frac{1}{3}(\Delta R_a + \Delta R_b + \Delta R_c) + \frac{1}{6}(2\Delta R_a - \Delta R_b - \Delta R_c) cos(2\theta_m) + \frac{\sqrt{3}}{6}(\Delta R_b - \Delta R_c) sin(2\theta_m)$$

$$R_{r12} = -\frac{1}{6}(2\Delta R_a - \Delta R_b - \Delta R_c) sin(2\theta_m) + \frac{\sqrt{3}}{6}(\Delta R_b - \Delta R_c) cos(2\theta_m)$$

$$R_{r13} = \frac{1}{3}(2\Delta R_a - \Delta R_b - \Delta R_c) cos(\theta_m) - \frac{\sqrt{3}}{3}(\Delta R_b - \Delta R_c) sin(\theta_m)$$

$$R_{r21} = R_{r12}$$

$$R_{r22} = \frac{1}{3}(\Delta R_a + \Delta R_b + \Delta R_c) - \frac{1}{6}(2\Delta R_a - \Delta R_b - \Delta R_c) cos(2\theta_m) + \frac{\sqrt{3}}{6}(\Delta R_b - \Delta R_c) sin(2\theta_m)$$

$$R_{r23} = -\frac{1}{3}(2\Delta R_a - \Delta R_b - \Delta R_c) sin(\theta_m) - \frac{\sqrt{3}}{3}(\Delta R_b - \Delta R_c) cos(\theta_m)$$

$$R_{r31} = \frac{1}{2} R_{r13}$$

$$R_{32} = \frac{1}{2} R_{r23}$$

$$R_{r33} = \frac{1}{3}(\Delta R_a + \frac{1}{3}(\Delta R_a + \Delta R_b + \Delta R_c)$$

D-APPENDIX: Motor Parameters:

Rated Power	3hp
Rated Voltage	230v
Rated Current	9A
Rotor Resistance	0.816Ω
Stator Resistance	0.435Ω
Magnetization Inductance	0.0695H
Stator Inductance	0.0024H
Rotor Inductance	0.0024H
Moment of Inertia	0.089 kgm^2
Load Torque	15Nm
Amount of Rotor Bars	28

ACKNOWLEDGMENT

This research received no external funding.

REFERENCES

[1] Saad, N., Irfan, M., & Ibrahim, R. (2018). Condition monitoring and faults diagnosis of induction motors: electrical signature analysis. CRC Press.

[2] Thomson, W. T., & Fenger, M. (2001). Current signature analysis to detect induction motor faults. IEEE Industry Applications Magazine, 7(4), 26-34.

[3] Karmakar, S., Chattopadhyay, S., Mitra, M., & Sengupta, S. (2016). Induction motor fault diagnosis: approach through current signature analysis. Singapore: Springer.

[4] Siddique, A., Yadava, G. S., & Singh, B. (2005). A review of stator fault monitoring techniques of induction motors. IEEE transactions on energy conversion, 20(1), 106-114.

[5] Bonnett, A. H., & Soukup, G. C. (1992). Cause and analysis of stator and rotor failures in three-phase squirrel-cage induction motors. IEEE Transactions on Industry applications, 28(4), 921-937.

[6] Mehrjou, M. R., Mariun, N., Marhaban, M. H., & Misron, N. (2011). Rotor fault condition monitoring techniques for squirrel-cage induction machine—A review. Mechanical Systems and Signal Processing, 25(8), 2827-2848.

[7] Sizov, G. Y., Yeh, C. C., & Demerdash, N. A. (2009, May). Magnetic equivalent circuit modeling of induction machines under stator and rotor fault conditions. In 2009 IEEE International Electric Machines and Drives Conference (pp. 119-124). IEEE.

[8] Hur, J., Toliyat, H. A., & Hong, J. P. (2001). Dynamic analysis of linear induction motors using 3-D equivalent magnetic circuit network (EMCN) method. Electric Power Components and Systems, 29(6), 531-541.

[9] Sudhoff, S. D., Kuhn, B. T., Corzine, K. A., & Branecky, B. T. (2007). Magnetic equivalent circuit modeling of induction motors. IEEE Transactions on Energy Conversion, 22(2), 259-270.

[10] Faiz, J., Ebrahimi, B. M., Akin, B., & Toliyat, H. A. (2007). Finite-element transient analysis of induction motors under mixed eccentricity fault. IEEE transactions on magnetics, 44(1), 66-74.

[11] Vaseghi, B., Takorabet, N., & Meibody-Tabar, F. (2009). Transient finite element analysis of induction machines with stator winding turn fault. Progress In Electromagnetics Research, 95, 1-18.

[12] Luo, X., Liao, Y., Toliyat, H. A., El-Antably, A., & Lipo, T. A. (1995). Multiple coupled circuit modeling of induction machines. IEEE Transactions on industry applications, 31(2), 311-318.

[13] Omar, T., Lahcene, N., Rachild, I., & Maurice, F. (2005, November). Modeling of the induction machine for the diagnosis of rotor defects. Part I. An approach of magnetically coupled multiple circuits. In the 31st Annual Conference of IEEE Industrial Electronics Society, 2005. IECON 2005. (pp. 8-pp). IEEE.

[14] OYMAN SERTELLER, N. F., Mergen, A. F., & Gizher, E., (2004). Time harmonic effects for rotor slot design considering deep bar squirrel cage induction motors . 9th International Conference on Optimization of Electrical and Electronic Equipment (pp.141-144). Brasov, Romania

[15] Williamson, S., & Mirzoian, K. (1985). Analysis of cage induction motors with stator winding faults. IEEE transactions on power apparatus and systems, (7), 1838-1842.

[16] Toliyat, H. A., & Lipo, T. A. (1995). Transient analysis of cage induction machines under stator, rotor bar and end ring faults. IEEE Transactions on Energy Conversion, 10(2), 241-247.

[17] Joksimovic, G. M., & Penman, J. (2000). The detection of inter-turn short circuits in the stator windings of operating motors. IEEE Transactions on Industrial Electronics, 47(5), 1078-1084.

[18] Jung, J. H., & Kwon, B. H. (2006). Corrosion model of a rotor-bar-under-fault progress in induction motors. IEEE Transactions on Industrial Electronics, 53(6), 1829-1841.

[19] Tang, J., Chen, J., Dong, K., Yang, Y., Lv, H., & Liu, Z. (2019). Modeling and evaluation of stator and rotor faults for induction motors. Energies, 13(1), 133.

[20] Patel, D. C., & Chandorkar, M. C. (2013). Modeling and analysis of stator interturn fault location effects on induction machines. IEEE transactions on industrial electronics, 61(9), 4552-4564.

[21] Maraaba, L., Al-Hamouz, Z., & Abido, M. (2018). An efficient stator inter-turn fault diagnosis tool for induction motors. Energies, 11(3), 653.

[22] Cruz, S. M., & Cardoso, A. M. (2005). Multiple reference frames theory: A new method for the diagnosis of stator faults in three-phase induction motors. IEEE Transactions on Energy Conversion, 20(3), 611-619.

[23] Chen, S., & Živanović, R. (2010). Modelling and simulation of stator and rotor fault conditions in induction machines for testing fault diagnostic techniques. European Transactions on Electrical Power, 20(5), 611-629.

[24] Santos, P. M., Correa, M. B. R., Jacobina, C. B., Da Silva, E. R. C., Lima, A. M. N., Didiery, G., ... & Lubiny, T. (2006, June). A simplified induction machine model to study rotor broken bar effects and for detection. In 2006

37th IEEE Power Electronics Specialists Conference (pp. 1-7). IEEE.
[25] Rahmatullah, R., Demir, M. F., & Serteller, N. F. O. (2020, October). Asenkron Motorların DQ Eksende Üç Referans Çerçevesinde Matlab/Simulink ile İncelenmesi. In 2020 Innovations in Intelligent Systems and Applications Conference (ASYU) (pp. 1-6). IEEE.
[26] Terron-Santiago, C., Martinez-Roman, J., Puche-Panadero, R., & Sapena-Bano, A. (2021). A Review of Techniques Used for Induction Machine Fault Modelling. Sensors, 21(14), 4855.
[27] Xianrong Chang, V. Cocquempot and C. Christophe, "A model of asynchronous machines for stator fault detection and isolation," in IEEE Transactions on Industrial Electronics. 50 (2003), 578-584.
[28] Bellini, A., Filippetti, F., Franceschini, G., Tassoni, C., & Kliman, G. B. (2001). Quantitative evaluation of induction motor broken bars by means of electrical signature analysis. IEEE Transactions on industry applications, 37(5), 1248-1255.

Contribution of Individual Authors to the Creation of a Scientific Article (Ghostwriting Policy)

Rohullah Rahmatullah contributed to the processing of the data and the writing of the article, Necibe Fusun Oyman Serteller contributed to the processing of the data and the writing of the article and Vedat Topuz contributed to the processing of the data and the writing of the article